

## 2.0 Introduction

We will now start discussing the properties of matter in the density range relevant to neutron stars, whose cross section is schematically illustrated in fig.1. Throughout these lectures we will always assume that neutron star matter be at  $T = 0^\circ\text{K}$  and transparent to neutrinos. The first assumption is justified by the fact that the typical neutron star temperature is  $\sim 10^9 \text{ }^\circ\text{K}$ , to be compared to an average kinetic energy of neutrons in the star interior in the range  $10^{11}\text{-}10^{12} \text{ }^\circ\text{K}$ . The second assumption is supported by the calculated values of the neutrino mean free path in neutron matter,  $\lambda >> 10 \text{ Km}$ , largely exceeding the typical neutron star radius.

This lecture is focused on the region of subnuclear density, i.e.  $\rho < \rho_0 = 2 \times 10^{14} \text{ g/cm}^3$ , corresponding to the outer and inner crust of the star. At densities above  $10^7 \text{ g/cm}^3$  and temperature below  $10^8 \text{ }^\circ\text{K}$ , matter is expected to be a solid, because the Coulomb interaction between ions is only weakly screened, and the Coulomb energy is minimized by a Body Centered Cubic (BCC) lattice.

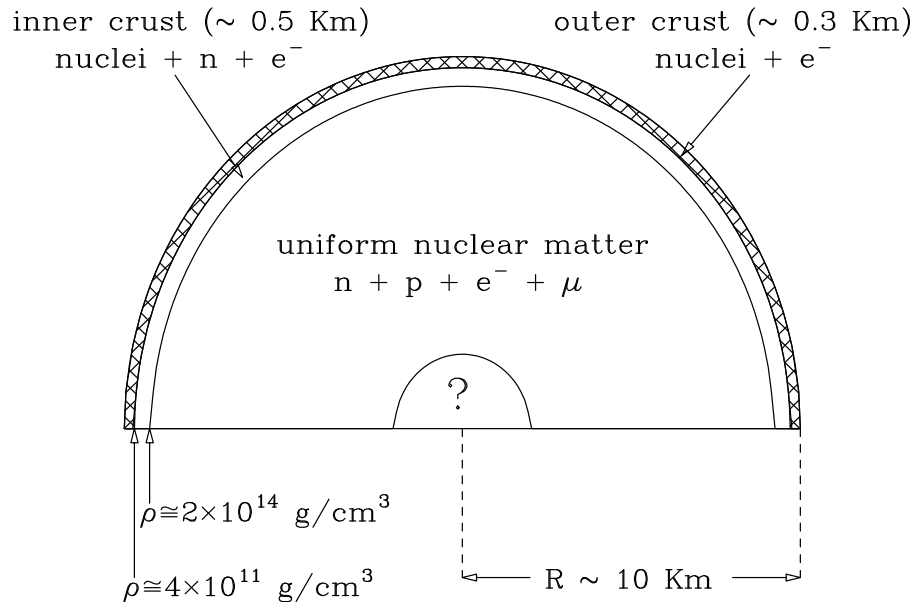


FIG. 1. Schematic representation of a neutron star's cross section.

Requiring that the fluctuation of the ions be small compared to average ion spacing  $r_z$ , one finds that a solid is expected to form at temperature  $T < T_m = Z^2 e^2 / (100 r_z)$ . In the case of  $^{56}\text{Fe}$ , solidification occurs at density  $\sim 10^7 \text{ g/cm}^3$ . As the density further increases,  $r_z$  decreases, so that the condition for solidification continues to be fulfilled. However, the large kinetic energy of the relativistic electrons shifts the energy balance, favouring inverse  $\beta$ -decay that leads to the appearance of neutron rich nuclei.

At density  $\sim 4 \times 10^{11} \text{ g/cm}^3$ , the neutrons produced by electron capture are barely bound, the nuclide with the largest neutron excess being  $^{118}\text{Kr}$ . This density correspond to the boundary between outer and inner crust of the neutron star (see figure). At larger density the neutrons are produced in positive energy states: they are said to *drip* out of the nuclei. As a consequence, the inner crust consist of a lattice of nuclei surrounded by a gas of electrons and neutrons.

## 2.1 Inverse $\beta$ -decay and neutronization

The neutronization process is due to the occurrence of inverse  $\beta$ -decay (i.e. electron capture), turning protons into

neutrons through:

$$p + e^- \rightarrow n + \nu_e . \quad (1)$$

Assuming neutrinos to be massless and non interacting, the above process is energetically allowed as soon as the electron energy becomes equal to  $c^2$  times the neutron-proton mass difference

$$\Delta mc^2 = m_n c^2 - m_p c^2 = 939.565 - 938.272 = 1.293 \text{ MeV} . \quad (2)$$

As a consequence, the electron number density at which inverse  $\beta$ -decay sets in can be estimated from

$$\sqrt{(p_F c)^2 + (m_e c^2)^2} = \Delta mc^2 , \quad (3)$$

where (see Lecture 1)

$$p_F = \hbar(3\pi^2 n_e)^{1/3} , \quad (4)$$

leading to

$$n_e = \frac{1}{3\pi^2} \left[ \frac{(\Delta mc^2)^2 - (m_e c^2)^2}{(\hbar c)^2} \right]^{3/2} \approx 7 \times 10^{30} \text{ cm}^{-3} . \quad (5)$$

The corresponding mass density for a fully ionized helium plasma, having  $Y_e = 0.5$ , is  $\rho \approx 2.4 \times 10^7 \text{ g/cm}^3$ .

Let us consider a system of protons, electrons and neutrons in equilibrium through inverse  $\beta$ -decay at temperature  $T = 0$ . All interactions, except the weak interaction, will be neglected. Process (1) obviously conserves the baryon number  $N_B$  (i.e. baryon number density) and electric charge. Hence

$$n_e = n_p , \quad (6)$$

implying in turn ( $p_{F,e}$  and  $p_{F,p}$  denote the electron and proton Fermi momentum, respectively)

$$p_{F,e} = p_{F,p} , \quad (7)$$

and

$$n_p + n_n = n_B = \frac{N_B}{\Omega} . \quad (8)$$

The requirement of equilibrium implies ( $\epsilon_n$ ,  $\epsilon_p$  and  $\epsilon_e$  denote the energy densities of neutrons, protons and electrons, respectively)

$$\frac{\partial \epsilon}{\partial n_n} = \frac{\partial}{\partial n_n} (\epsilon_n + \epsilon_p + \epsilon_e) = 0 . \quad (9)$$

From ( $\alpha = n, p, e$ )

$$\begin{aligned} \sum_{\alpha} \frac{\partial \epsilon_{\alpha}}{\partial n_n} &= \sum_{\alpha} \frac{2}{(2\pi)^3} \frac{1}{\hbar^3} \left( \frac{\partial p_{F,\alpha}}{\partial n_n} \right) \frac{\partial}{\partial p_{F,\alpha}} 4\pi \int_0^{p_{F,\alpha}} p^2 dp \sqrt{(pc)^2 + (m_{\alpha} c^2)^2} \\ &= \sum_{\alpha} \frac{8\pi}{(2\pi)^3} \frac{1}{\hbar^3} \left( \frac{\partial p_{F,\alpha}}{\partial n_n} \right) p_{F,\alpha}^2 \sqrt{(p_{F,\alpha} c)^2 + (m_{\alpha} c^2)^2} \end{aligned} \quad (10)$$

and (use  $n_p = n_B - n_n = n_e$ )

$$\frac{8\pi}{(2\pi)^3} \frac{1}{\hbar^3} \left( \frac{\partial p_{F,\alpha}}{\partial n_n} \right) p_{F,\alpha}^2 = \begin{cases} +1 & \text{for } \alpha = n \\ -1 & \text{for } \alpha = e, p \end{cases} , \quad (11)$$

we finally get

$$\frac{\partial \epsilon}{\partial n_n} = \sqrt{(p_{F,n} c)^2 + (m_n c^2)^2} - \sqrt{(p_{F,p} c)^2 + (m_n c^2)^2} - \sqrt{(p_{F,e} c)^2 + (m_e c^2)^2} = 0 . \quad (12)$$

The above equations is nothing but the condition for chemical equilibrium, that can be rewritten in terms of the chemical potentials  $\mu_\alpha = (\partial\epsilon_\alpha/\partial n_\alpha)$  as

$$\mu_n = \mu_p + \mu_e . \quad (13)$$

Eq.(13), together with the requirement of charge neutrality (eq.(7)), completely specifies the equation of state of a mixture of non interacting protons, electrons and neutrons in equilibrium at  $T = 0$ . For any given matter density  $\rho$  we can write

$$\rho = \rho_B = \rho_p + \rho_n \quad (14)$$

and define the proton and neutron fractions

$$x_p = \frac{\rho_p}{\rho} \quad (15)$$

and

$$x_n = \frac{\rho_n}{\rho} = 1 - x_p . \quad (16)$$

Substitution of eq.(7) into eq.(13) then yields an equation for  $x_n$ .

Once the value of  $x_n$  is known, the neutron, proton and electron number densities can be evaluated and the pressure

$$P = P_n + P_p + P_e \quad (17)$$

can be obtained using eq.(23) of Lecture 1. Fig. 2 shows the proton and neutron number densities,  $n_p$  and  $n_n$  (remember:  $n_e = n_p$ ) as a function of matter density  $\rho$ .

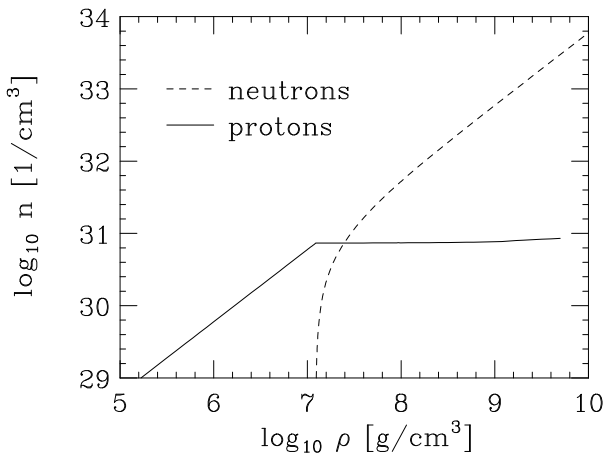


FIG. 2. Number density of noninteracting protons and neutrons in  $\beta$ -equilibrium as a function of matter density.

It can be seen that in the range  $10^5 \leq \rho \leq 10^7 \text{ g}/\text{cm}^3$  there are protons only and  $\log(n_p)$  grows linearly with  $\log(\rho)$ . At  $\rho \sim 10^7 \text{ g}/\text{cm}^3$  neutronization sets in and the neutron number density begins to steeply increase. At  $\rho > 10^7$   $n_p$  stays nearly constant, while neutrons dominate.

The equation of state of the  $\beta$ -stable mixture is shown in fig. 3. Its main feature is that pressure remains nearly constant as matter density increases by almost two orders of magnitude, in the range  $10^7 \leq \rho \leq 10^9 \text{ g}/\text{cm}^3$ . The electron and neutron contributions to the pressure are shown in fig. 4. Note that, since charge neutrality requires  $n_p = n_e$ , the proton pressure is smaller than the electron pressure by a factor  $(m_p/m_e) \sim 2000$ .

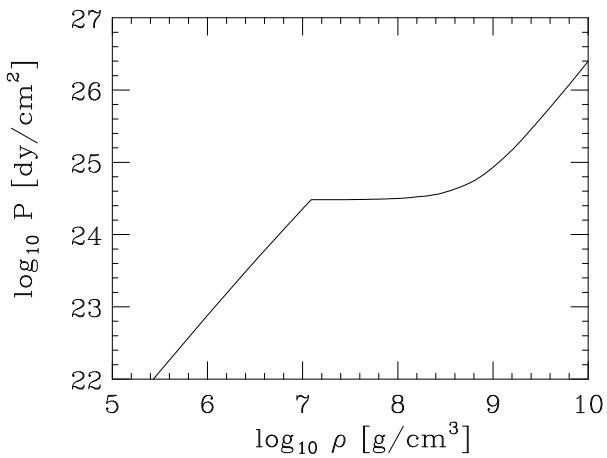


FIG. 3. Equation of state of a mixture of noninteracting neutrons electrons and protons in  $\beta$ -equilibrium.

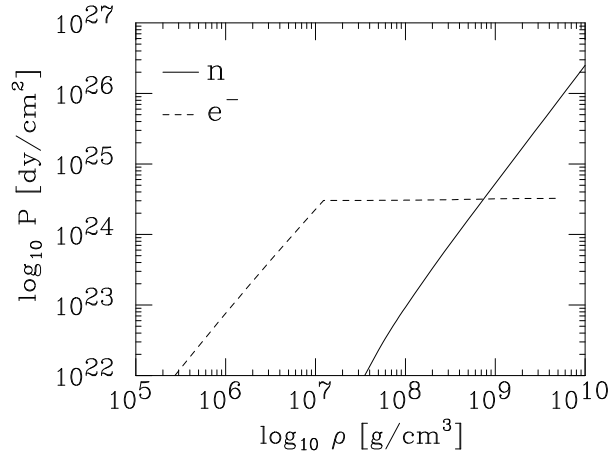


FIG. 4. Density dependence of the neutron and electron contributions to the pressure of  $\beta$ -stable matter.

## 2.2 Nuclear semi-empirical mass formula and stability of neutron-rich nuclei

The description of  $\beta$ -stable matter in terms of a mixture of degenerate Fermi gases of neutrons, protons and electrons is strongly oversimplified. In reality, electron capture changes a nucleus with given charge  $Z$  and mass number  $A$  into a different nucleus with the same  $A$  and charge ( $Z-1$ ). Moreover, the new nucleus may be metastable, so that two-step processes of the type



can take place. Chemical equilibrium is driven by the mass difference between neighboring nuclei rather than the neutron-proton mass difference.

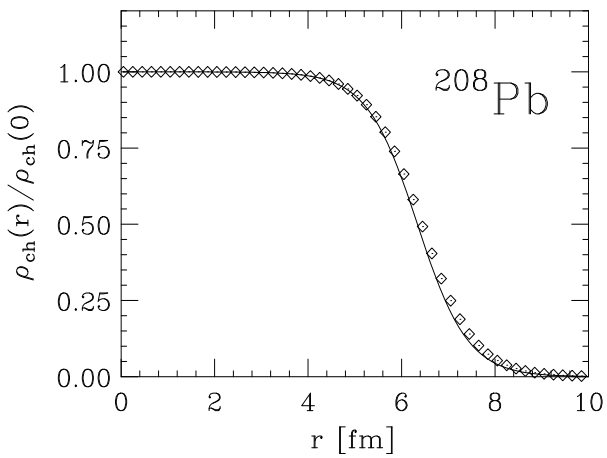


FIG. 5. Nuclear charge distribution of  $^{208}Pb$ , normalized to  $Z/\rho(0)$  ( $Z = 82$ ). The solid line has been obtained using the parametrization of eq.(19), while the diamonds represent the results of a model independent analysis of electron scattering data.

The measured nuclear masses,  $M(Z, A)$ , and charge distributions exhibit two very important features:

- The charge density is nearly constant within the nuclear volume, its value being roughly the same for all stable nuclei, and drops from  $\sim 90\%$  to  $\sim 10\%$  of the maximum over a distance  $T \sim 2.5$  fm ( $1$  fm =  $10 \times 10^{-13}$  cm), independent of  $A$ , called surface thickness (see fig. 5). It can be parametrized in the form

$$\rho_{ch}(r) = \rho_0 \frac{1}{1 + e^{(r-R)/D}} , \quad (19)$$

where  $R = r_0 A^{1/3}$ , with  $r_0 = 1.07$  fm, and  $D = 0.54$  fm. Note that the nuclear charge radius is proportional to  $A^{1/3}$ , implying that the nuclear volume increases linearly with the mass number  $A$ .

- The (positive) binding energy per nucleon, defined as

$$\frac{B(Z, A)}{A} = \frac{1}{A} [Zm_p c^2 + (A - Z)m_n c^2 + Zm_e c^2 - M(Z, A)] , \quad (20)$$

where  $M(Z, A)$  is the measured nuclear mass, is almost constant for  $A \geq 12$ , its value being  $\sim 8.5$  MeV (see fig. 6).

The  $A$  and  $Z$  dependence of  $B(Z, A)$  can be parametrized according to the *semiempirical-mass formula*

$$\frac{B(Z, A)}{A} = \frac{1}{A} \left[ a_V A - a_s A^{2/3} - a_c \frac{Z^2}{A^{1/3}} - a_A \frac{(A - 2Z)^2}{4A} + \lambda a_p \frac{1}{A^{1/2}} \right] . \quad (21)$$

The first term in square brackets, proportional to  $A$ , is called the *volume term* and describes the bulk energy of nuclear matter. The second term, proportional to the nuclear radius squared, is associated with the surface energy, while the third one accounts for the Coulomb repulsion between  $Z$  protons uniformly distributed within a sphere of radius  $R$ . The fourth term, that goes under the name of *symmetry energy* is required to describe the experimental fact that stable nuclei tend to have the same number of neutrons and protons. Moreover, even-even nuclei (i.e. nuclei having even  $Z$  and even  $N = A - Z$ ) tend to be more stable than even-odd or odd-odd nuclei. This property is accounted for by the last term in the above equation, where  $\lambda = -1, 0$  and  $+1$  for even-even, even-odd and odd-odd nuclei, respectively. Figure 6 shows the different contributions to  $B(Z, A)/A$ , evaluated using eq.(21).

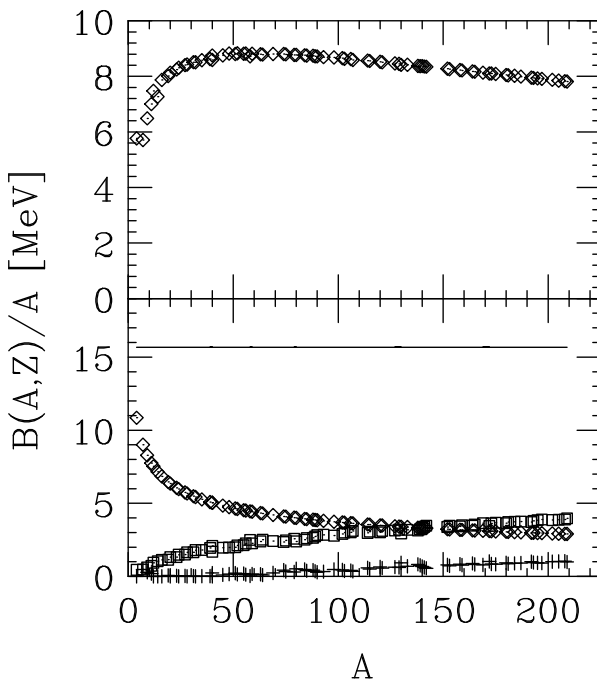


FIG. 6. Upper panel: A-dependence of the binding energy per nucleon of stable nuclei, evaluated according to eq.(21) with  $a_V = 15.67$  MeV,  $a_s = 17.23$  MeV,  $a_c = .714$  MeV,  $a_A = 93.15$  MeV and  $a_p = 11.2$  MeV. Lower panel: the solid line shows the magnitude of the volume contribution to the binding energy per nucleon, whereas the A-dependence of the surface, coulomb and symmetry contributions are represented by diamonds, squares and crosses, respectively.

The semi-empirical nuclear mass formula of eq.(21) can be used to obtain a qualitative description of the neutronization process. The total energy density of the system consisting of nuclei of mass  $A$  and charge  $Z$  arranged in a lattice and surrounded by a degenerate electron gas is

$$\epsilon_T(n_B, A, Z) = \epsilon_e + \left( \frac{n_B}{A} \right) [M(Z, A)c^2 + \epsilon_L] , \quad (22)$$

where  $\epsilon_e$  is the energy of the electron gas, given by eq.(24) of Lecture 1,  $n_B$  and  $(n_B/A)$  denote the number densities of nucleons and nuclei, respectively, and  $\epsilon_L$  is the electrostatic lattice energy per site. As a first approximation, the contribution of  $\epsilon_L$  will be neglected.

At any given nucleon density  $n_B$  the equilibrium configuration corresponds to the values of  $A$  and  $Z$  that minimize  $\epsilon_T(n_B, A, Z)$ , i.e. to  $A$  and  $Z$  such that

$$\left( \frac{\partial \epsilon_T}{\partial Z} \right)_{n_B} = 0 , \quad \left( \frac{\partial \epsilon_T}{\partial A} \right)_{n_B} = 0 . \quad (23)$$

Combining the above relationships and using eq.(21) one finds

$$Z \simeq 3.54 A^{1/2} . \quad (24)$$

Once  $Z$  is known as a function of  $A$ , any of the two relationships (23) can be used to obtain  $A$  as a function of  $n_B$ . The mass number  $A$  turns out to be an increasing function of  $n_B$ , implying that  $Z$  also increases with  $n_B$ , but at a slower rate. Hence, nuclei become more massive and more and more neutron rich as the nucleon density increases.

The above discussion is obviously oversimplified. In reality,  $A$  and  $Z$  are *not* continuous variables and the total energy has to be minimized using the nuclear masses, rather than the parametrization of eq.(21), and including the lattice energy, that can be written as

$$\epsilon_L = -K \frac{(Ze)^2}{r_s} \quad (25)$$

where  $r_s$  is related to the number density of nuclei through  $(4\pi/3)r_s^3 = (n_B/A)^{-1}$  and  $K = 0.89593$  for a BCC lattice, yielding the lowest energy. At fixed nucleon number density  $n_B$  we can write the total energy density in the form

$$\epsilon_T(n_B, A, Z) = \epsilon_e + \left( \frac{n_B}{A} \right) \left[ M(Z, A)c^2 - 1.4442(Ze)^2 \left( \frac{n_B}{A} \right)^{1/3} \right], \quad (26)$$

where, for matter density exceeding  $\sim 10^6$  g/cm<sup>3</sup>, the extreme relativistic limit of the energy density of an electron gas at number density  $n_e = Zn_B/A$  (see Lecture 1) has to be used to evaluate  $\epsilon_e$ :

$$\epsilon_e = \frac{3}{4} (\hbar c) \left( Z \frac{n_B}{A} \right)^{4/3}. \quad (27)$$

Collecting together the results of eqs.(25)-(27) and expressing  $n_B$  in units of  $n_{B_0} = 10^{-9}$  fm<sup>-3</sup> (the number density corresponding to a matter density  $\sim 10^6$  g/cm<sup>3</sup>), the total *energy per nucleon*,  $\epsilon_T/n_B$ , can be rewritten in units of MeV as

$$\frac{\epsilon_T}{n_B} = \frac{M(Z, A)c^2}{A} + \frac{1}{A^{4/3}} \left[ 0.4578 Z^{4/3} - \frac{Z^2}{480.74} \right] \left( \frac{n_B}{n_{B_0}} \right)^{1/3}. \quad (28)$$

The average energy per nucleon in a nucleus is about 930 MeV. It can be conveniently written in units of MeV in the form  $M(Z, A)c^2/A = 930 + \Delta$ . As long as we are dealing with nuclides that are not very different from the stable nuclides, the values of  $\Delta$  are available in form of tables based on actual measurements or extrapolations from the experimental data.

In practice,  $\epsilon_T/n_B$  of eq.(28) is computed for a given nucleus (i.e. for given  $A$  and  $Z$ ) as a function of  $n_B$ , and plotted versus  $1/n_B$  (see fig. 7). The curves corresponding to different nuclei are then compared and the nucleus corresponding to the minimum energy at given  $n_B$  can be easily picked out. For example, the curves of fig. 7 show the behavior of the energy per particle corresponding to <sup>62</sup>Ni and <sup>64</sup>Ni, having  $N = (A-Z) = 34$  and 36, respectively. It is apparent that a first order phase transition is taking place around the point where the two curves cross one another. The exact densities at which the phase transition occurs and terminates can be obtained using Maxwell's double tangent construction. This method essentially amounts to drawing a straight line tangent to the convex curves associated with the two nuclides. In a first order phase transition the pressure remains constant as the density increases. Hence, as all points belonging to the tangent of Maxwell's construction correspond to the same pressure, the onset and termination of the phase transition are simply given by the points of tangency. As expected, at higher density the nucleus with the largest number of neutrons yields a lower energy.

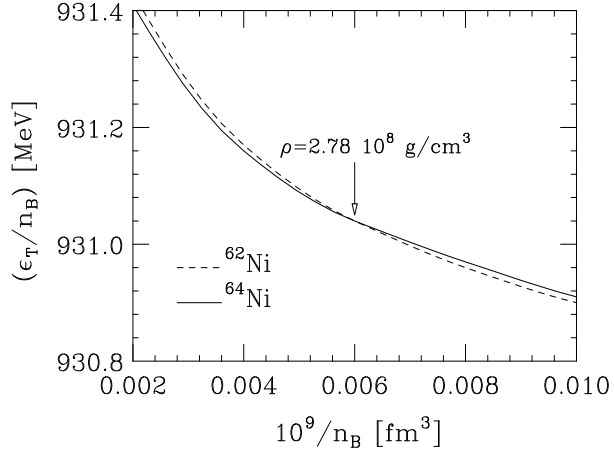


FIG. 7. Total energy per nucleon of a BCC lattice of <sup>62</sup>Ni (dashed line) and <sup>64</sup>Ni (solid line) nuclei surrounded by an electron gas, evaluated using eq.(28) and plotted versus the inverse nucleon number density.

It has to be pointed out that there are limitations to the approach described in this section. Some of the nuclides entering the minimization procedure have ratios  $Z/A$  so different from those corresponding to stable nuclei (whose typical value of  $Z/A$  is  $\sim 0.5$ ) that the accuracy of the extrapolated masses may be questionable. Obviously, this problem becomes more and more important as the density increases. The study of nuclei far from stability, carried out with radioactive nuclear beams, is regarded as one of the highest priorities in nuclear physics research, and new dedicated experimental facilities are currently being planned both in the U.S. and in Europe.

Table I reports the sequence of nuclides corresponding to the ground state of matter at subnuclear density, as a function of matter density.

Nuclide	Z	N = A - Z	Z/A	$\Delta$ [MeV]	$\rho_{max}$ [g/cm <sup>3</sup> ]
<sup>56</sup> Fe	26	30	.4643	.1616	$8.1 \times 10^6$
<sup>62</sup> Ni	28	34	.4516	.1738	$2.7 \times 10^8$
<sup>64</sup> Ni	28	36	.4375	.2091	$1.2 \times 10^9$
<sup>84</sup> Se	34	50	.4048	.3494	$8.2 \times 10^9$
<sup>82</sup> Ge	32	50	.3902	.4515	$2.1 \times 10^{10}$
<sup>84</sup> Zn	30	54	.3750	.6232	$4.8 \times 10^{10}$
<sup>78</sup> Ni	28	50	.3590	.8011	$1.6 \times 10^{11}$
<sup>76</sup> Fe	26	50	.3421	1.1135	$1.8 \times 10^{11}$
<sup>124</sup> Mo	42	82	.3387	1.2569	$1.9 \times 10^{11}$
<sup>122</sup> Zr	40	82	.3279	1.4581	$2.7 \times 10^{11}$
<sup>120</sup> Sr	38	82	.3166	1.6909	$3.7 \times 10^{11}$
<sup>118</sup> Kr	36	82	.3051	1.9579	$4.3 \times 10^{11}$

TABLE I. Sequence of nuclei corresponding to the ground state of matter and maximum density at which they occur. Nuclear masses are given by  $M(Z,A)c^2/A = (930 + \Delta)$  MeV.

### 2.3 Neutron drip

Table I shows that as the density increases the nuclides corresponding to the ground state of matter become more and more neutron rich. At  $\rho \sim 4.3 \times 10^{11}$  g/cm<sup>3</sup> the ground state corresponds to a Coulomb lattice of <sup>118</sup>Kr nuclei, having proton to neutron ratio  $\sim 0.31$  and a slightly negative neutron chemical potential (i.e. neutron Fermi energy), surrounded by a degenerate electron gas with chemical potential  $\mu_e \sim 26$  MeV. At larger densities a new regime sets in, since the neutrons created by electron capture occupy positive energy states and begin to *drip* out of the nuclei, filling the space between them.

At these densities the ground state corresponds to a mixture of two phases: matter consisting of neutron rich nuclei (phase I), with density  $\rho_{nuc}$ , and a neutron gas of density  $\rho_{NG}$  (phase II).

The equilibrium conditions are

$$(\mu_n)_I = (\mu_n)_{II} = \mu_n \quad (29)$$

and

$$\mu_p = \mu_n - \mu_e , \quad (30)$$

where  $(\mu_n)_I$  and  $(\mu_n)_{II}$  denote the neutron chemical potential in the neutron gas and in the matter of nuclei, respectively.

The details of the ground state of matter in the neutron drip regime are specified by the densities  $\rho$ ,  $\rho_{nuc}$  and  $\rho_{NG}$ , the proton to neutron ratio of the matter in phase I and its surface, whose shape is dictated by the interplay between surface and Coulomb energies.

Recent studies suggest that at densities  $4.3 \times 10^{10} \lesssim \rho \lesssim .75 \times 10^{14}$  g/cm<sup>3</sup> the matter in phase I is arranged in spheres immersed in electron and neutron gas, whereas at  $.75 \times 10^{14} \lesssim \rho \lesssim 1.2 \times 10^{14}$  g/cm<sup>3</sup> the energetically favoured configurations exhibit more complicated structures, featuring rods of matter in phase I or alternating layers of matter in phase I and phase II. At  $\rho \gtrsim 1.2 \times 10^{14}$  g/cm<sup>3</sup> there is no separation between the phases, and the ground state of matter corresponds to a homogeneous fluid of neutrons, protons and electrons.